BIOCHEMISTRY
including biophysical chemistry & molecular biology
Article

Biochemistry **2010,** *49,* 2627–2635 2627
DOI: 10.1021/bi901913a

Kinetic Analysis of the Interaction of b/HLH/Z Transcription Factors Myc, Max, and Mad with Cognate DNA[†]

Ozgur Ecevit, Mateen A. Khan, and Dixie J. Goss*

Department of Chemistry and Biochemistry, Hunter College and Graduate Center of the City University of New York, New York, New York 10065

Received November 6, 2009; Revised Manuscript Received January 25, 2010

ABSTRACT: Myc, Mad, and Max proteins belong to the basic helix−loop−helix leucine zipper family of transcription factors. They bind to a specific hexanucleotide element of DNA, the E-box (CACGTG). To be biologically active, Myc and Mad require dimerization with Max. For the route of complex assembly of these dimers, there are two proposed pathways. In the monomer pathway, two monomers bind DNA sequentially and assemble their dimerization interface while bound to DNA. In the dimer pathway, two monomers form a dimer first prior to association with DNA. The monomer pathway is kinetically favored. In this report, stopped-flow polarization was utilized to determine the rates and temperature dependence of all of the individual steps for both assembly pathways. Myc·Max dimerization had a rate constant ∼5- and ∼2-fold higher than those of Max·Max and Mad·Max dimerization, respectively. The protein dimerization rates as well as the dimer−DNA rates were found to be independent of concentration, suggesting conformational changes were rate-limiting. The Arrhenius activation energies for the dimerization of Myc, Mad, and Max with Max were 20.4 ± 0.8, 29 ± 0.6, and 40 ± 0.2 kJ/mol, respectively. Further, rate constants for Max·Max homodimer DNA binding are significantly higher than for Myc·Max and Mad·Max heterodimers binding to DNA. Monomer−DNA binding showed a faster rate than dimer−DNA binding. These studies show the rate-limiting step for the dimer pathway is the formation of protein dimers, and this reaction is slower than formation of protein dimers on the DNA interface, kinetically favoring the monomer pathway.

Myc, Max, and Mad are members of the basic helix−loop−helix leucine zipper family of transcription factors. Myc was first discovered as the protooncogene of avian retroviruses inducing lymphoid tumors (*1*). It is believed to regulate 15% of all genes (*2*). Deregulation of Myc has been implicated in the development of many human cancers, including Burkitt lymphoma, neuroblastomas, small cell lung cancers, breast cancers, esophageal cancer, adenocarcinoma, and meduloblastomas (*3*, *4*). c-Myc is overexpressed in neoplasia by a number of different mechanisms, including gene amplification, translocation, retroviral insertion, and activation of pathways upstream of c-Myc expression (*5*). The Myc family proteins, c-Myc, n-Myc, and l-Myc, have been implicated almost exclusively in cell proliferation, differentiation, and neoplasia (*6*−*10*). However, recent advances have shown that c-Myc is involved in a wide catalog of cellular activity, which includes recruitment to the transcriptosome of a variety of transcriptional effectors, including TRRAP (transformation/transcription) domain-associated protein, Miz1 (transcriptional repressor), and the E2 ubbiquin ligase Skp2, and activates the cad gene that encodes the trifunctional enzyme carbamoyl-phosphate synthase/aspartate transcarbamoylase/dehydroorotase, which is required for the first three rate-limiting steps of pyrimidine biosynthesis (*11*−*13*).

Since neither dimerization nor DNA-specific binding could be readily demonstrated for Myc protein, a search for Myc interacting proteins led to the identification of Max protein. The Myc-obligate factor X, Max, is a b/HLH/Z[1] family protein similar to Myc but lacks the transactivation domain. Max can also form homodimers. Studies showed that it may act as a transcription repressor in a homodimer form (*14*). All known oncogene functions of Myc require dimerization with Max. The Myc·Max transcription activator is involved in the transcriptional regulation of target genes associated with cellular growth, proliferation, metabolism, and differentiation (*7*, *15*). The fact that Max is expressed in the absence of Myc led to searches for other partners that interact with Max. Mad family proteins were all identified in expression cloning screens by their ability to bind specifically to Max (*16*−*18*). Like Myc, Mad homodimerizes poorly but interacts with Max, forming a sequence-specific DNA binding complex similar to the Myc·Max heterodimer. Overexpression of Mad in tissue culture and mice interferes with cell proliferation and inhibits transformation (*15*). Mad and Myc compete for binding to Max.

The X-ray crystal structures of the b/HLH/Z domains of Myc·Max and Mad·Max heterodimers revealed that both heterodimers bind to their common DNA target, the enhancer

[†]This work was supported in part by National Science Foundation Grants MCB 0413982 and MCB 0814051 (to D.J.G.). Infrastructure at Hunter College is supported by National Institutes of Health Research Center in Minority Institution Award RR-03037.

*To whom correspondence should be addressed: Department of Chemistry, Hunter College, City University of New York, New York, NY 10065. Telephone: (212) 772-5383. Fax: (212) 772-5332. E-mail: dgoss@hunter.cuny.edu.

[1]Abbreviations: b/HLH/Z, basic helix−loop−helix leucine zipper; DNA E-box, 6 bp double-stranded DNA CACGTG sequence known as the enhancer box; MLP, major late promoter; LCR, human β-globin locus control region; FITC, fluorescein isothiocyanate; IPTG, isopropyl β-D-thiogalactopyranoside; EDTA, ethylenediaminetetraacetic acid; DTT, dithiothreitol; PBS, phosphate-buffered saline; HEPES, 4-(2-hydroxyethyl)-1-piperazineethanesulfonic acid; SDS, sodium dodecyl sulfate; DMSO, dimethyl sulfoxide.

Published on Web 02/19/2010

box (E-box) hexanucleotide (5′-CACGTG-3′) (*8*, *19*). E-Boxes are located in the proximal region of class II nuclear gene promoters, between 50 and 200 bp upstream of the transcription sites. Binding of these structurally similar transcription factor dimers to the E-box determines whether a cell will divide and proliferate (Myc·Max) or differentiate and become quiescent (Mad·Max). Many transcriptional factors form dimeric complexes with DNA (*20*, *21*). In the absence of DNA, they may be found as either monomers (*22*) or dimers (*23*). The homodimer or heterodimer of Max·Max, Myc·Max, and Mad·Max transcription factors recognized the DNA E-box (*24*). The discrimination between the cognate and nonspecific Max b/HLH/Z/DNA complex has been reported using EMSA, CD, and NMR techniques (*25*, *26*) and crystal structures using X-ray crystallography (*27*) . Mass spectrometry or proteolysis has also been employed to characterize the binding of Max to specific and nonspecific DNA (*28*).

Given the ever-expanding catalog of c-Myc functions as a transcription factor, we in this laboratory ascertained that few quantitative data were available regarding the thermodynamic cycle of how the Myc/Max/Mad network behaves in relation to their protein−protein interactions and the E-box. In this study, as in our previous work, the b/HLH/Z domains of Myc and Max and full-length Mad1 were studied (see Experimental Procedures). In our first study, Hu et al. (*29*) using fluorescence anisotropy showed that specific binding between MLP DNA and Max had an affinity ∼10-fold higher than that of LCR DNA and ∼100-fold higher than that for nonspecific DNA. USF had a binding affinity similar to that of Max for MLP DNA (*29*, *30*), but Max bound more tightly to LCR and nonspecific DNA. A series of E-box alterations showed for Max binding that most of the energy involved could be attributed to the two halves of the E-box showing virtually no cooperativity. Measurement of binding for the entire thermodynamic cycle of monomer−dimer−DNA interactions showed that the monomer−Max−DNA complex exhibited a significantly reduced affinity for the second monomer of Max. Our work showed that the Myc·Max heterodimer formed the most stable heterodimer. Further, Banerjee et al. (*46*) also from this laboratory showed that formation of a dimer complex might be affected by a general environment with respect to charge. Thus, by fluorescence anisotropy, it was shown that poly-L-lysine had insignificant effects and poly-L-glutamic acid stabilized both homodimers and heterodimers. These results showed that dimerization of all three monomers in a negatively charged milieu was driven by both negative enthalpy and entropic contributions. van der Waals and H-bonding interactions are most likely at play in the formation of these complexes.

Kinetic analysis has shown that assembly of the dimeric transcription factors (bZIP and bHLHZip) and specific DNA sites follows a pathway in which two protein monomers bind DNA sequentially and form their dimerization interface while bound to DNA (monomer pathway) (*31*). The individual steps of this process provide kinetic control which will lead to different intermediates that can interact at different rates with other proteins and nonspecific DNA and ultimately allow for discrimination between specific and nonspecific DNA. Therefore, it is important to determine the rate-limiting steps and kinetics of the individual steps in an attempt to understand regulation of transcription by cellular and viral proteins and other pharmacological agents.

In this work, stopped-flow anisotropy techniques were utilized to study the dimerization kinetics of Max, Myc, and Mad in the absence and presence of the DNA E-box. The rate constants for Myc·Max, Mad·Max, and Max·Max dimerization and the temperature dependence of these reactions were measured and compared. Our kinetic data showed that Myc·Max dimerization is faster than Max·Max or Mad·Max dimerization. The Myc, Max, and Mad dimerization rates were found to be independent of concentration, suggesting conformational changes are rate-limiting. To understand the assembly of transcription complex, we analyzed whether Myc or Mad competes to form a heterodimer with Max at the DNA E-box. Further, we measured and compared the dimer−DNA and monomer−DNA binding rate of the individual steps in the assembly pathway (monomer/dimer pathway) and determined the activation energies of the reactions.

EXPERIMENTAL PROCEDURES

Materials. GST-bind resin and the HiTrap SP column were obtained from Amersham Pharmacia Biotech, Inc. His-bind Ni resin was purchased from Novagen, an affiliate of Merck Co. Ltd. Sephadex G-25 was purchased from Pharmacia Fine Chemicals Inc. (Piscataway, NJ). Fluorescein isothiocyanate (FITC) was obtained from Molecular Probes, Inc. Oligonucleotides used in these studies were synthesized on a 200 nmol scale by Gene Link (Hawthorne, NY). Fluorescein was attached at the 5′ end of the 16-mer oligonucleotides during the synthesis.

Expression and Purification of Proteins. Expression vectors Max/pET3a and c-Myc/pGEX2T were kindly provided by SK Burley, SGX Pharmaceuticals, Inc. (San Diego, CA). Cloning vector pET30a containing the full-length Mad cDNA was purchased from Open Biosystems (Huntsville, AL). All three vectors were transformed into *Escherichia coli* BL21(DE3) pLysS cells that express T7 RNA polymerase from the IPTG-inducible lacUV5 promoter. Truncated proteins Max and c-Myc consisting of amino acids 22−113 and 347−439, respectively, and full-length Mad1 contained the functional b/HLH/Z domains (*16*, *27*, *32*) . Cells containing pET Max or pGEX Myc were selected by colony selection and inoculated into 1 L of LB medium with 100 μg/mL ampicillin and grown at 37 °C until the OD_{600} reached 0.5−1. The culture was induced with 1 mM isopropyl β-D-thiogalactopyranose (IPTG), and the growth of the culture was allowed to continue for 6 h at 30 °C. Cells were harvested by centrifugation for 20 min at 6000 rpm and resuspended in lysis buffer [20 mM HEPES buffer (pH 7.6), 0.5 mM PMSF, 10% glycerol, protease inhibitor cocktail, and lysozyme] and sonicated for 2 min with a 30 s interval. The lysed cells were centrifuged at 18000 rpm for 15 min to separate soluble proteins from inclusion bodies (Myc and Mad1). The supernatant was used for the purification of the Max protein using ion exchange chromatography.

The inclusion bodies for Mad1 were isolated from cell lysates and washed twice with 10 mL of 20 mM HEPES buffer (pH 7.6) containing 1% Triton X-100. After centrifugation at 18000 rpm for 30 min, the inclusion bodies were dissolved in 2 mL of 50 mM HEPES buffer (pH 7.6), 6 M guanidine hydrochloride, and 25 mM DTT and incubated for 1 h at 4 °C. To pellet the insoluble material, the sample was centrifuged at 18000 rpm for 10 min and the supernatant was diluted into 20 mL of 50 mM HEPES (pH 7.6).

The inclusion bodies for c-Myc were washed as described above for Mad1. The inclusion bodies were solubilized with 10 mL of phosphate-buffered saline (PBS) (pH 7.4) containing 1% Triton X-100 and incubated overnight with gentle stirring.

After removal of the insoluble material by centrifugation, the soluble protein was diluted into 20 mL of 20 mM cold PBS (pH 7.4).

HiTrap SP ion exchange chromatography was used for the purification of Max. c-Myc was purified by GST affinity chromatography using 20 mM PBS (pH 7.4) as the wash buffer and 200 mM Tris-HCl (pH 8.5) containing 50 mM glutathione as the elution buffer. GST was enzymatically removed from Myc. The purification of Mad1 was performed on a Ni^{2+}-His trap affinity column. The column was prepared according to the manufacturer's instructions and washed with 10 volumes of binding buffer [20 mM Tris-HCl (pH 7.9) containing 0.5 M NaCl and 5 mM imidazole]. The supernatant containing the Mad protein was loaded on the affinity column. The column was washed with an additional 10 volumes of wash buffer [20 mM Tris-HCl (pH 7.9) containing 0.5 M NaCl and 60 mM imidazole], and the bound protein was eluted with elution buffer [20 mM Tris-HCl (pH 7.9) containing 0.5 M NaCl and 1 M imidazole]. The protein fractions were collected and dialyzed against HEPES buffer (pH 7.6). The purity of all three proteins was determined by 10% SDS−polyacrylamide gel electrophoresis. After the proteins had been concentrated with Centricon YM filters (Amicon Co.), the concentrations of protein were determined with a Bradford assay with bovine serum albumin as the standard (*33*) using a Bio-Rad protein assay reagent (Bio-Rad Laboratories, Hercules, CA). Protein purity was estimated to be >98% by examination of serial dilutions via SDS−polyacrylamide gel electrophoresis (*34*) and Coomassie Blue staining. Proteins were stored in small aliquots to prevent repeated thawing and frozen at −70 °C in storage buffer [10% glycerol, 1 mM PMSF, 100 mM KCl, 5 mM Hepes-KOH (pH 7.5), and 10 mM DTT]. No difference in activity (EMSA) was detected between freshly prepared and frozen samples. Electrophoretic mobility shift assays (EMSA) with E-box-containing oligonucleotides demonstrated high-affinity, specific DNA binding activity for Myc·Max and Mad·Max heterodimers (data not shown and ref *19*).

Fluorescent Labeling of Max. Fluorescein isothiocyanate (FITC) reacts only with uncharged primary amines of proteins to form dye−protein conjugates. Therefore, the N-terminus of Max was labeled with FITC as follows. The concentration of purified Max was adjusted to 1 mg/mL in 50 mM HEPES buffer (pH 7.6). In the labeling procedure, 100 μL of a 1.5 mg/mL reactive dye stock solution [dissolved in anhydrous dimethyl sulfoxide (DMSO)] is added to 1 mL of protein solution. The FITC-labeled Max mixture was incubated overnight at 4 °C with gentle agitation and protected from light. FITC-labeled Max was purified on a Sephadex G-25 column equilibrated with 50 mM HEPES buffer (pH 7.6). The FITC-conjugated protein fractions were collected in the void volume and concentrated with Centricon YM filters (Amicon Co.) by centrifugation for 6 h at 4000 rpm. To determine the concentration, the purified protein was diluted into HEPES buffer and the absorbance at both 280 and 494 nm was measured. The absorption and fluorescence emission maxima of FITC-labeled proteins were 494 and 518 nm, respectively. The final protein concentration was calculated according to the formula protein concentration = $[(A_{280} - 0.30A_{494}) \times \text{dilution factor}]/\varepsilon$, where 0.30 is a correction factor (CF) and ε is the molar extinction coefficient of the protein at 280 nm. CF = $(A_{280}$ free dye$)/(A_{494}$ free dye) = 0.30 for FITC. The CF is included to compensate for absorption of the dye at 280 nm. The degree of labeling was calculated using an ε of 68000 M^{-1} cm^{-1} for FITC. Labeled Max is termed Max-FITC. Max-FITC competed with unlabeled Max for DNA binding, showing labeling did not perturb the protein binding (*29*).

DNA Oligonucleotides. The 16 bp oligonucleotide used in this study contained the sequence derived from the adenovirus major late promoter (MLP) containing the E-box (CACGTG). The DNA duplex contained the sequence 5′-TAGGCCACGTGACCGG-3′ and its complementary strand. Complementary strands were annealed together to form duplex DNA. Each DNA strand (labeled oligonucleotide and unlabeled complement) at 20 μM was dissolved in nuclease-free water, heated to 75−80 °C for 30 min, and allowed to cool at room temperature.

Stopped-Flow Anisotropy Measurements. Stopped-flow fluorescence anisotropy experiments were performed with an OLIS RSM 1000 stopped-flow spectrophotometer equipped with a fluorescence polarization module. The dead time of the stopped-flow system, the age of the mixture when it is first available for measurement, is 1 ms. The instrument was configured in T-format, and emission was collected through 495 nm cut-on filters (provided by ORIEL Corp., Stratford, CT) placed in front of each photomultiplier tube. A 450 W Xe arc lamp with a single grating monochromator was used. The excitation wavelength for FITC-labeled Max protein (^{FITC}Max) was 490 nm. A temperature-controlled circulating water bath was used to maintain the temperature of the flow cell and solution reservoirs. After the samples had been rapidly mixed, the time course of fluorescence anisotropy change was recorded by computer data acquisition. All measurements were conducted in titration buffer consisting of 20 mM HEPES-KOH (pH 7.6), 0.5 mM $MgCl_2$, and 1 mM DTT containing 150 mM KCl. One thousand data points were collected per rapid-mix shot. For each experiment, the data from 6−10 shots were averaged to improve the signal-to-noise ratio. Each averaged set of stopped-flow data was then analyzed by nonlinear least-squares fitting equations using Kaleidagraph (Synergy Software, West Palm Beach, FL). Data from the anisotropy experiments were fitted to the single- and double-exponential functions as described previously (*35*, *36*). Fitted curves correspond to the following single-exponential equation

$$r_{(t)} = r_0 + Ae^{-k_{obs}t} \quad (1)$$

where $r_{(t)}$ is the anisotropy observed at any time t, r_0 is the anisotropy when the reaction reaches equilibrium,and A is the amplitude. k_{obs} is the observed first-order rate constant. The kinetic data for the double-exponential equation are

$$r_{(t)} = r_0 + A_1e^{-k_{obs1}t} + A_2e^{-k_{obs2}t} \quad (2)$$

where A_1 and A_2 are the amplitudes $[r_{(t)} - r_0]$ for the first and second components of double-exponential reactions with observed rate constants k_{obs1} and k_{obs2}, respectively. The residuals were measured by the differences between the calculated fit and the experimental data. All the reactions in this study were consistent with a single-exponential process. Arrhenius plots were constructed by using the observed rate constants at different temperatures according to the equation

$$\ln k = (-E_a/RT) + \ln A \quad (3)$$

where k is the rate constant, E_a is the activation energy, R is the universal gas constant, T is the absolute temperature, and A is the Arrhenius pre-exponential factor. Activation energies were calculated using the slopes of ln k versus $1/T$ (kelvin).

Under pseudo-first-order conditions, stopped-flow experiments were conducted using high concentrations of Max, Myc, and Mad and limiting concentrations of FITC-labeled Max to ensure that the bimolecular combination of ^{FITC}Max with unlabeled protein was pseudo-first-order. The mechanisms considered involved a one- and two-step binding process (*37*).

For a one-step model

$$M + M \underset{k_{-1}}{\overset{k_1}{\rightleftharpoons}} D \quad (4)$$

where M and D are the monomer and dimer protein, respectively; k_1 and k_{-1} are the forward and reverse rate constants, respectively. Under the pseudo-first-order condition, the observed rate constant is predicted to be a linear function of substrate concentration, i.e., $k_{obs} = k_1[C] + k_{-1}$.

For a two-step model

$$M + M \underset{k_{-1}}{\overset{k_1}{\rightleftharpoons}} D* \underset{k_{-2}}{\overset{k_2}{\rightleftharpoons}} D \quad (5)$$

where M is the monomeric protein, D* is an intermediate, and D is the final complex. The model involves the fast association of monomer protein followed by a slow change in conformation of the first association complex (D*) to the stable complex (D), giving rise to fluorescence anisotropy change. The binding rates have the following relationship, assuming $k_2 \gg k_{-2}$ with the concentration of substrate: $1/k_{obs} = 1/k_2 + K_1/k_2[C]$ as described previously (*30*, *38*), where k_{obs} is the observed first-order rate constant, k_2 is the forward rate constant for the second step, K_1 is the equilibrium constant for the first step, and [C] is the concentration of dimeric protein. A plot of $1/k_{obs}$ versus 1/[C] will give an intercept of $1/k_2$.

RESULTS

The Kinetics of Heterodimer Formation Are Faster than Those of the Homodimer Protein. The stopped-flow data for the dimerization of transcription factors Max, Myc, and Mad with FITC-labeled Max were plotted as the anisotropy change versus time as shown in Figure 1. Stopped-flow kinetic traces were fitted to a single- and double-exponential equation using nonlinear regression analysis as described in Experimental Procedures. The kinetic data showed that ^{FITC}Max·Myc binding ($k_2 = 90 \pm 4\ s^{-1}$) and ^{FITC}Max·Mad binding ($k_2 = 44 \pm 1.1\ s^{-1}$) were ~4.5- and ~2.2-fold faster, respectively, than ^{FITC}Max·Max binding ($k_2 = 20 \pm 0.5\ s^{-1}$) (Figure 1 and Table 1). Treatment of the data using a double-exponential function did not improve the fit (data not shown). The residuals representing the deviation between the calculated and experimental data (Figure 1, bottom panel) indicate that the single-exponential function fits the points over the entire time course of measurements.

Under the pseudo-first-order conditions, where unlabeled protein (Max, Myc, or Mad) was in excess, the observed pseudo-first-order rate constant is predicted to be a linear function of the concentration of ^{FITC}Max. To test this prediction, Myc·Max, Mad·Max, and Max·Max dimerization experiments were performed over a concentration range of 0.2−2 μM, a 4−40-fold excess. In all these experiments, the concentration of the FITC-labeled Max was kept constant at 50 nM. According to K_d values (*29*) of Myc, Mad, and Max interactions, 90% of the Max forms a dimer with Myc and Mad. Figure 2 shows the rate constants of the Max·Max, Myc·Max, and Mad·Max interactions at different concentrations. The Max, Myc, and Mad dimerization rates were found to be nearly independent of concentration, suggesting conformational changes are rate-limiting.

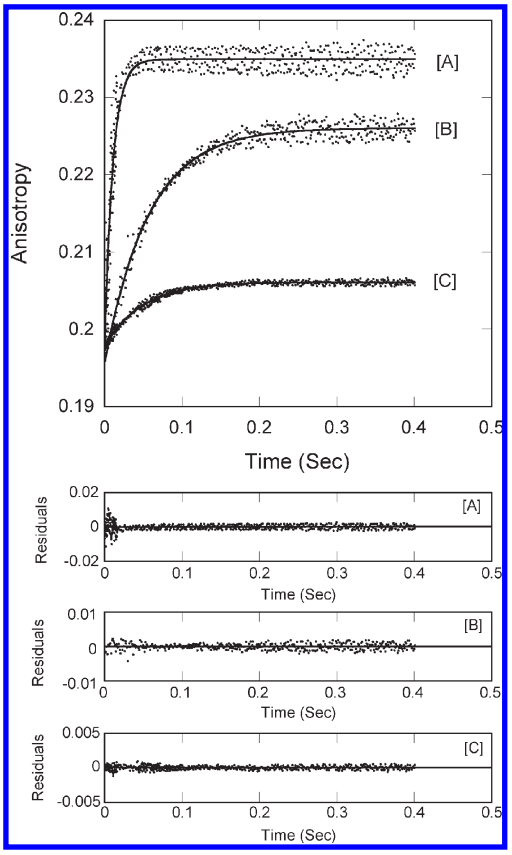

FIGURE 1: Stopped-flow kinetic measurements of binding of Max, Myc, and Mad to FITC-labeled Max protein. Representative kinetic data show the time-dependent increase in anisotropy after 50 nM ^{FITC}Max (final concentration) had been mixed with 0.2 μM unlabeled (final concentration) (A) Myc, (B) Mad, and (C) Max at 21 °C. Residuals for the fits are shown in the bottom panels. The experimental conditions are described in Experimental Procedures.

Table 1: Kinetic Binding Constants for the Interaction of Transcription Factors Max, Myc, and Mad with FITC-Labeled Max

	association rate constant, k_{obs} (s^{-1})		
temp (°C)	Max·Max	Max·Myc	Max·Mad
13	11.1 ± 0.4	67 ± 2	32.2 ± 0.7
21	20 ± 0.5	90 ± 4	44 ± 1.1
27	22.1 ± 0.4	109 ± 4.0	55.4 ± 1.5
32	30 ± 0.7	118 ± 7	65 ± 5
E_a (kJ/mol)	40 ± 0.2	20.4 ± 0.8	29 ± 0.6

For a model involving a conformational change, explained in Experimental Procedures, the binding rates have a relationship with the concentration of substrate as described previously (*30*, *38*): $1/k_{obs} = 1/k_2 + K_1/k_2[C]$, where k_{obs} is the observed first-order rate constant, k_2 is the forward rate constant for the second step, K_1 is the equilibrium constant for the first step, and [C] is the concentration of the unlabeled protein Max, Myc, or Mad. The $1/k_{obs}$ versus 1/[C] plots shown in Figure 2 for Max·Max, Myc·Max, and Mad·Max dimerization confirm the predicted linear relationship. k_2 values, obtained from the intercept, were found to be 20 ± 1.1, 91 ± 2.3, and 44.3 ± 1.4 s^{-1} for

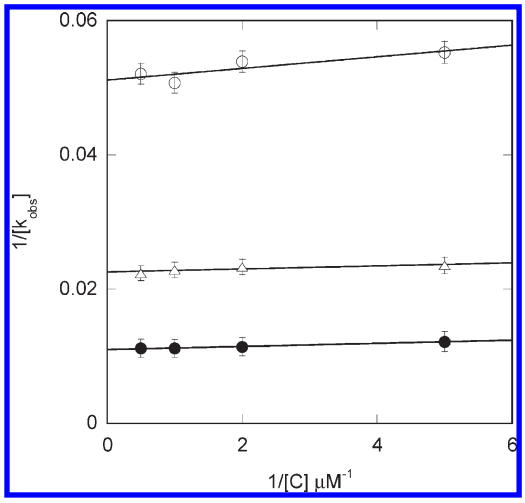

FIGURE 2: Kinetic plots of $1/k_{obs}$ vs $1/[C]$ for the interaction of 50 nM ^{FITC}Max with varying concentrations of Max (○), Myc (●), and Mad (△). Rate constant k_2 was obtained as the reciprocal of the y-intercept.

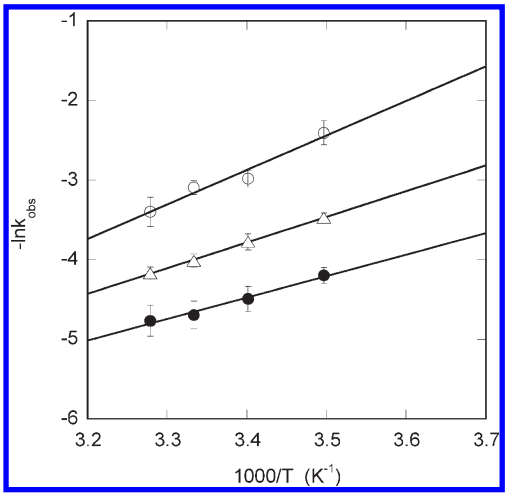

FIGURE 3: Arrhenius plots for the interaction of Max, Myc, and Mad with ^{FITC}Max. The rate constant values for Max (○), Myc (●), and Mad (△) with ^{FITC}Max protein at different temperatures were used to construct an Arrhenius plot according to eq 5. The activation energy was calculated from the slope of the fitted linear plot of ln k vs T^{-1} (kelvin).

Max·Max, Myc·Max, and Mad·Max dimerization, respectively.

Rate constants for all three protein−protein interactions, Max, Myc, and Mad binding to ^{FITC}Max, at different temperatures are listed in Table 1. The stopped-flow kinetic data revealed that at all four temperatures Myc·Max dimerization had the highest rate constants compared to the other two transcription factor dimerizations. Myc·Max interaction had a rate constant 4.0−6-fold higher than that of Max·Max homodimerization and 2.0-fold higher than that of Max·Mad dimerization. The values of k_2 for Max, Myc, and Mad binding to ^{FITC}Max at different temperatures were calculated from the data sets collected at each temperature (Table 1) as a representative plot shown in Figure 1.

The rate constants in Table 1 were used to construct Arrhenius plots (Figure 3) according to eq 3. The activation energies were obtained from the slope of the linear fit of ln k versus $1/T$ plots. Our results show that the activation energies for the Max·Myc and Max·Mad heterodimers are ∼2.0- and 1.4-fold lower, respectively, than that for the Max·Max homodimer. The overall lower activation energy for heterodimer binding suggests a number of more favorable hydrogen bonds are formed in the transition state.

Homodimer Protein Binds to DNA Faster Than Heterodimer Protein. To determine the DNA binding rate constants of the Max·Max homodimer and Myc·Max and Mad·Max heterodimers, stopped-flow anisotropy experiments were performed using 16-mer 5′-FITC-labeled DNA E-box oligonucleotide. In all these kinetic studies, the final concentration of the 5′-FITC-labeled 16-mer DNA oligonucleotide was kept constant at 50 nM. Varying concentrations of the unlabeled Max·Max, Myc·Max, and Mad·Max protein dimers were injected into the mixing chamber of the stopped-flow instrument; 0.2 μM Max was preincubated with 2 μM Myc or Mad protein at room temperature for 30 min prior to the reaction with the DNA E-box. K_d values (*29*) for the protein−protein interactions were used to calculate protein dimer formation; 91% of the Myc·Max and Mad·Max heterodimers were in the dimer form at a protein mixing concentration of 200 nM. The stopped-flow data for the binding of FITC-labeled 16-mer DNA with Max·Max, Max·Myc, and Max·Mad protein complexes were plotted as the anisotropy versus time as shown in Figure 4. The changes in

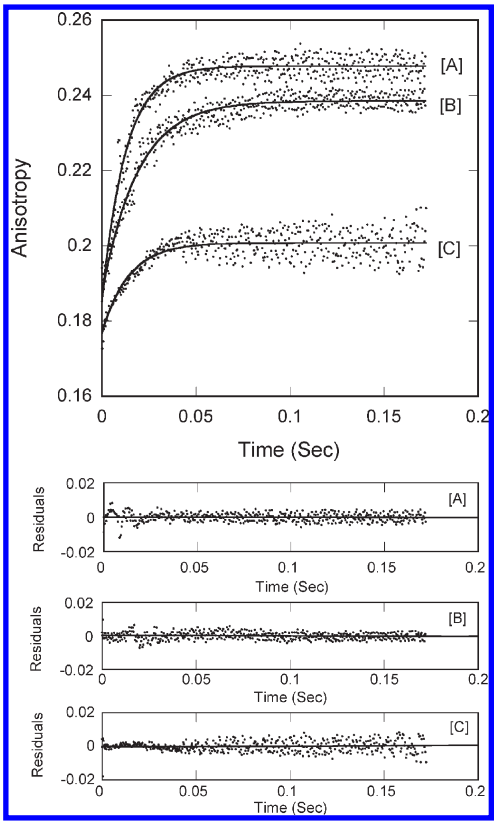

FIGURE 4: Stopped-flow kinetic measurements of binding of Max·Max, Myc·Max, and Mad·Max protein dimers to the FITC-labeled 16-mer DNA E-box. Representative kinetic data show the time-dependent increase in anisotropy after rapid mixing of 50 nM ^{FITC}DNA E-box (final concentration) with 0.2 μM unlabeled (final concentration) (A) Max·Max (B) Max·Myc, and (C) Max·Mad at 21 °C. Residuals for the fits are shown in the bottom panels. The experimental conditions are described in Experimental Procedures.

the anisotropy as a function of time for the three different protein dimers binding to E-box DNA were recorded, and data were fitted using nonlinear regression analysis as a single and double exponential (eqs 1 and 2). Max·Max binding (k_{obs} = 132 ± 7.4 s^{-1}) showed a rate constant ∼2-fold higher than that of

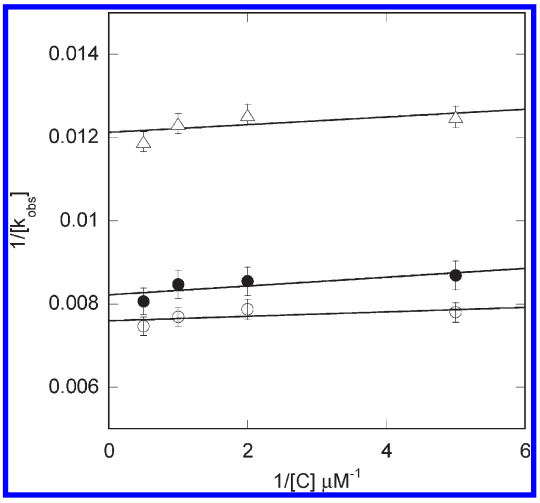

FIGURE 5: Kinetic plots of $1/k_{obs}$ vs 1/[C] for the interaction of 50 nM ^{FITC}DNA E-box with varying concentrations of Max·Max (○), Max·Myc (●), and Max·Mad (△) dimer protein. Rate constant k_2 was obtained as the reciprocal of the *y*-intercept.

Table 2: Kinetic Binding Constants for the Interaction of Max·Max, Max·Myc, and Max·Mad Transcription Factors with the DNA E-Box

	association rate constant, k_{obs} (s^{-1})		
temp (°C)	Max·Max−DNA	Max·Myc−DNA	Max·Mad−DNA
13	116 ± 5.0	103 ± 5	60.4 ± 6
21	132 ± 7.4	118 ± 2.4	78 ± 2
27	147 ± 8.0	127 ± 8.4	86 ± 3
32	151 ± 5	144 ± 6.2	98 ± 1.5
E_a (kJ/mol)	10.5 ± 0.5	12.0 ± 0.4	20 ± 0.3

Max·Mad binding (k_{obs} = 78 ± 2 s^{-1}) for binding to the DNA E-box (Figure 4). Myc·Max binding rate constants were similar to the Max·Max binding rate constants. Treatment of the data using a double-exponential function did not improve the fit (data not shown).

To determine whether protein dimer−DNA rates are concentration-dependent, a $1/k_{obs}$ versus 1/[C] graph was plotted (Figure 5). The kinetic plots revealed that the interactions between the Max·Max, Myc·Max, and Mad·Max protein dimers and the DNA E-box are concentration-independent. From the intercept of $1/k_{obs}$ versus 1/[C], k_2 was found to be 133 ± 5, 122 ± 4.3, and 82 ± 4 s^{-1} for Max·Max−DNA, Myc·Max−DNA, and Mad·Max−DNA interactions, respectively.

The interactions between Max·Max, Myc·Max, and Mad·Max protein dimers and the FITC-labeled DNA E-box oligonucleotide were also investigated at different temperatures. The effects of the temperature on the rate constants of these protein dimer−DNA reactions are listed in Table 2. The final concentrations of the protein dimers and DNA E-box in the mixing chamber of the stopped-flow instrument were 0.2 μM (each) and 50 nM, respectively. The rate for the reaction of Max·Max and Myc·Max dimers is significantly faster than that of the Mad·Max dimer with the DNA E-box. From the temperature dependence of the rate constants of these dimer−DNA interactions, Arrhenius plots (Figure 6) were obtained and activation energies (E_a) were evaluated from their slopes. Analysis of the Arrhenius plots shows that the activation energies for Max·Max−DNA (E_a = 10.5 ± 0.5 kJ/mol) and Max·Myc−DNA

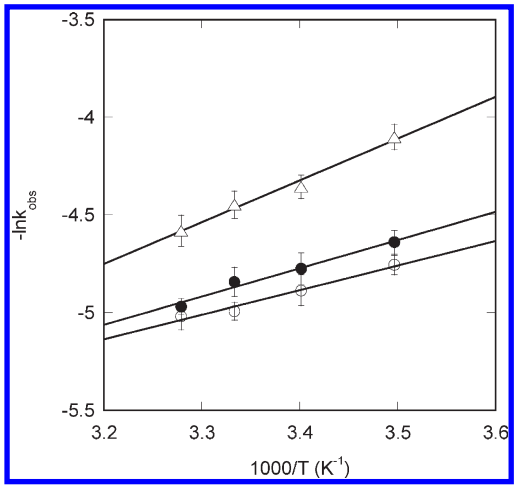

FIGURE 6: Arrhenius plots for the interaction of the ^{FITC}DNA E-box with Max·Max, Max·Myc, and Max·Mad dimer proteins. The rate constant values for Max·Max (○), Max·Myc (●), and Max·Mad (△) proteins at different temperatures were used to construct an Arrhenius plot according to eq 5. The activation energy was calculated from the slope of the fitted linear plot of ln *k* vs T^{-1} (kelvin).

(E_a = 12 ± 0.4 kJ/mol) interactions are very similar. The activation energy for the interaction of the Max·Mad dimer (E_a = 20 ± 0.3 kJ/mol) is ~2-fold higher than for Max·Max and Max·Myc dimers with the DNA E-box (Table 2).

Addition of a Second Monomer to the Monomer−DNA Complex Lowers the Rate. To compare the monomer− and dimer−DNA kinetics, we further studied the monomer−DNA kinetics. Max is the only protein among the three b/HLH/z family transcription factors (Myc, Max, and Mad) that has a significant affinity for DNA. The other two proteins, Myc and Mad, in the form of monomers, have a very low affinity for DNA (*15*). They form homodimers weakly and bind DNA poorly. Therefore, binding of monomeric Myc and Mad to DNA can be neglected. To avoid the DNA binding of dimeric Max proteins, we determined the most suitable experimental conditions using the previously published equilibrium data (*26*, *29*). To ensure that 90% of Max protein is in the monomeric form and not dimeric, the required concentration of Max protein was calculated using the K_d value (*29*) for the monomer−dimer equilibrium. To determine kinetic rates, 50 nM Max protein and 1 μM 16-mer DNA oligonucleotides were mixed in the stopped-flow mixing chamber, and the association rate constants were observed as shown in Figure 7. The association rate constant for binding of monomeric Max protein to the DNA E-box was 158 ± 4.4 s^{-1}. Binding of the second monomer (Myc) to form a heterodimer−DNA complex may serve to aid in selection of DNA. The association rate constantsfor the ·DNA complex with Max, Myc,and Mad were 138 ± 5, 126 ± 4.1, and 101 ± 4 s^{-1}, respectively. The monomer−DNA complex (Max−DNA; k_2 = 158 ± 4.4 s^{-1}) has a faster rate than the dimer−DNA complex.

Figure 8 shows the pathway for the formation of complexes of b/HLH/Z transcription factors (Max, Myc, and Mad) with DNA via a dimer and monomer pathway. In the dimer pathway, first proteins form dimers, which then bind to the DNA and form a dimer−DNA complex. In the monomer pathway, first a monomer binds to DNA and forms a monomer−DNA complex, followed by recruitment of the second monomer to form the final complex. Equilibrium 1 followed by equilibrium 2 is the dimer pathway. Equilibria 3 and 4 represent the monomer

pathway. The monomer and dimer pathways are energetically equivalent (thermodynamic cycle), and preference for one or the other is kinetic. Our kinetic data are very much in agreement with the proposed monomer−DNA binding pathway. Here we provide kinetic constants and show that dimer formation is the rate-limiting step in the dimer pathway, whereas both steps of the monomer pathway are rapid and have comparable rates.

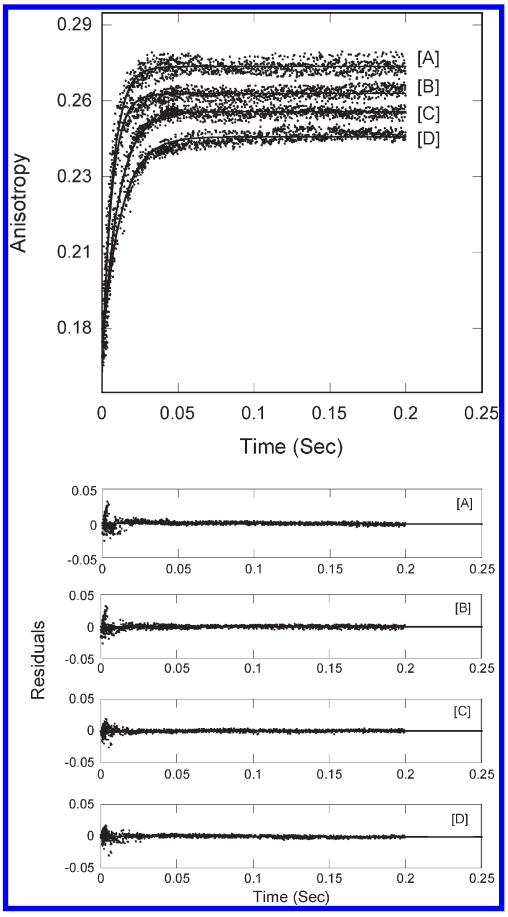

FIGURE 7: Kinetic measurements for the binding of monomer protein to the DNA E-box. Data show the time-dependent increase in anisotropy after (A) 50 nM ^{FITC}Max (final concentration) and 1 μM DNA E-box (final concentration), (B) Max−DNA complex and 1 μM Max, (C) Max−DNA complex and 1 μM Myc, and (D) Max−DNA complex and 1 μM Mad had been rapidly mixed at 21 °C.

DISCUSSION

In this study, we provide details of protein dimer−DNA kinetics, which form complexes with DNA via the monomer pathway. Previously, proteins belonging to b/Z (*39*, *40*) and b/HLH (*41*) nuclear hormone receptor (*22*) families, Arc (*42*), and LexA (*43*) repressors have been shown to bind DNA using the monomer pathway.

Stopped-flow fluorescence resonance energy transfer (FRET) studies conducted with cFos and cJun by Kohler and Schepartz (*39*) showed that although the dimerization of these proteins occurred rapidly in the absence of DNA, the rate of dimerization was enhanced in the presence of DNA. Their explanation for why the DNA binding is accelerated is based on electrostatic interactions between the proteins and DNA. Charge−charge interactions between the negatively charged DNA and positively charged proteins are the main attractive forces, which form the monomer−DNA interface (*44*). For Coulombic electrostatic interactions, the force between two molecules of opposite charges is proportional to the inverse of the separation distance squared. Thus, in the case of basic protein monomers and acidic DNA, one expects an accelerated binding. Our study showed that the rate of protein dimerization (step 1 in Figure 8) is limiting the overall rate of the dimer pathway (step 1 followed by step 2 in Figure 8). Therefore, the monomer pathway provides a faster route to the final complex. Another advantage of the monomer pathway lies in the fact that unfolded proteins (monomeric Max) have a larger capture radius than folded proteins (dimeric b/HLH/Z proteins) (*44*). Because of this larger capture radius, monomeric Max recognizes DNA with an increased rate. Studies showed that kinetics of binding of monomeric Fos and monomeric Jun to DNA provide a better fit to the experimental data than the dimer pathway (*39*). In a previous work published by Park et al. (*45*), the association kinetic constants of the interaction of truncated Max·Max and Myc·Max dimers with DNA were determined. Their results are also in good agreement with ours in terms of the similarity of the rate constants of Myc·Max and Max·Max dimers binding to DNA. They found that the Max·Max dimer recognized DNA at almost the same rate as the Myc·Max dimer, which was also the case in our study.

Previously, the binding and thermodynamic stability and specific DNA binding to the Myc, Max, and Mad family (*26*, *29*, *46*) were assessed. To fully understand the forces involved in

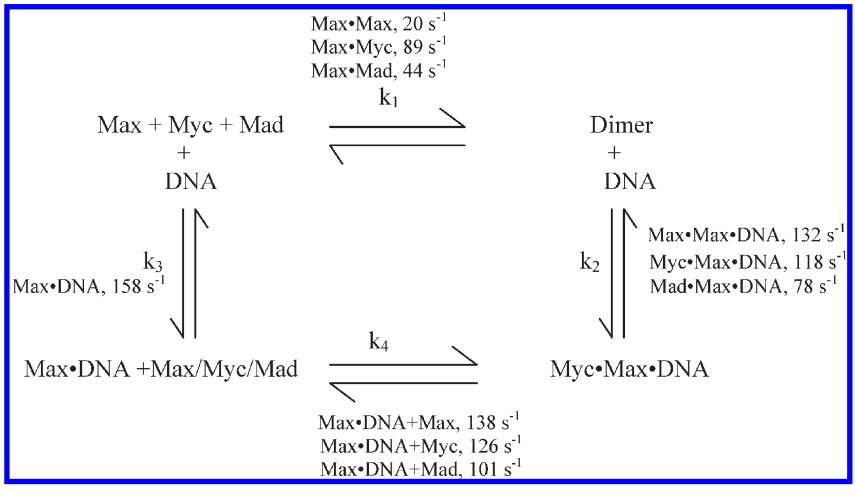

FIGURE 8: Schematic diagram of the Myc, Max, and DNA E-box interactions. The model shows the two pathways (k_1 with k_2 and k_3 with k_4) for the formation of the Myc·Max−DNA complex. The k values at different temperatures are listed in Tables 1 and 2.

protein−DNA recognition, we report the pre-steady state kinetic results for the interactions of the b/HLH/Z family transcription factors (Max, Myc, and Mad) with each other and also with DNA using stopped-flow anisotropy. The concentration dependencies of the observed rates of these processes correspond with a two-step reaction model in which initial fast formation of the dimer−DNA complex is followed by a conformational change of the complex in a rather fast step, but with a measurable rate.

In the case of formation of Myc·Max and Mad·Max heterodimers, the activation energy was lower compared to that of the Max·Max homodimer. This reduced temperature dependence suggests that the heterodimer interaction is accelerated and a substantially lower energy barrier is provided. The lower activation energy of the Max·Myc and Max·Mad dimerization suggests an intermediate that more easily achieves a stable conformation. Binding of Myc to the Max monomer has higher rate constants at all temperatures than formation of the Max·Max and Mad·Max dimers, suggesting that the Myc·Max complex is able to more rapidly change conformation.

It was observed that dimer−DNA interaction was concentration-independent. Binding of dimeric transcription factors to a 16-mer oligonucleotide exhibits two kinetic phases: initial rapid phase and a rather fast, concentration-independent phase. The reaction is interpreted as the concentration-dependent initial complex, which rearranges in a concentration-independent step to a thermodynamically stable complex. The rate for the interaction of the dimeric proteins with E-box DNA is faster than the rate of formation of the protein dimers, at all temperatures. The rates for the formation of Myc·Max−DNA and Max·Max−DNA complexes were higher than that of the Mad·Max−DNA complex. The Arrhenius activation energies for the binding of Max·Max and Myc·Max dimers is ~2-fold lower than that of the Max·Mad dimer binding to the DNA E-box.

The conclusions of a similar study by Kohler and Schepartz (*39*) suggest that assembly of dimeric transcription factors Jun-Fos and specific DNA follows the monomer pathway. However, Kohler and Schepartz preferred an experimental condition, in which the dimer−DNA complex was formed from monomeric Jun, monomeric Fos, and DNA. However, in a cellular environment, there are monomeric and also dimeric proteins presented that may compete for DNA. In such a case, the ratio of monomeric proteins to dimeric ones may be a crucial factor for determining the choice of the pathway. It is important to recognize that the assembly of transcription factor−DNA complexes in vivo is more intricate than in vitro. In the cellular environment, the transcription factors discriminate between specific and nonspecific DNA as well as a large excess of other proteins with which the transcription factors have to compete for DNA.

The most commonly discussed theory for DNA-binding proteins to recognize their specific sequences is "facilitated diffusion" (*47*). According to this theory, proteins find their target by sliding along the DNA. This is one-dimensional diffusion during which the protein remains in contact with the DNA for sufficiently long periods so that appreciable diffusive motion occurs in either direction along the chain contour. Since the unspecific DNA binding of a monomeric protein is weak compared to a dimeric one due to more interactions between the DNA, it may slide faster along the DNA. The diffusion rate of a monomeric protein may be more rapid because it is sterically less hindered. Therefore, one of the reasons why the monomer pathway is preferred over the dimer pathway may be the fast diffusion rate of the monomeric transcription factor along the DNA.

Another factor affecting the rate of target recognition is the stability of the protein−DNA complex. Accessory proteins may influence the stability of these complexes by binding to monomeric or dimeric transcription factors. Hence, the rate of DNA binding through a monomer or dimer pathway may differ depending on whether such accessory proteins bind to the monomeric or dimeric transcription factors. Future experiments will explore the effect of accessory proteins on the stability of these complexes and the diffusion rates of monomeric and dimeric transcription factors along the DNA.

REFERENCES

1. Duesberg, P. H., Bister, K., and Vogt, P. K. (1977) The RNA of avian acute leukemia virus MC29. *Proc. Natl. Acad. Sci. U.S.A. 74*, 4320–4324.
2. Gearhart, J., Pashos, E. E., and Prasad, M. K. (2007) Pluripotency redux-advances in stem-cell research. *N. Engl. J. Med. 357*, 1469–1472.
3. Boult, J. K., Taniere, P., Hallissey, M. T., Campbell, M. J., and Tselepis, C. (2008) Oesophageal adenocarcinoma is associated with a deregulation in the MYC/MAX/MAD network. *Br. J. Cancer 98*, 1985–1992.
4. MacGregor, D. N., and Ziff, E. B. (1990) Proteins of the Myc network: Essential regulators of cell growth and differentiation. *Pediatr. Res. 28*, 63–68.
5. Henriksson, M., and Luscher, B. (1996) Regulation of cyclin D2 gene expression by the Myc/Max/Mad network: Myc-dependent TRRAP recruitment and histone acetylation at the cyclin D2 promoter. *Adv. Cancer Res. 68*, 109–182.
6. Bouchard, C., Dittrich, O., Kiermaier, A., Dohmann, K., Menkel, A., Eilers, M., and Luscher, B. (2001) Regulation of cyclin D2 gene expression by the Myc/Max/Mad network: Myc-dependent TRRAP recruitment and histone acetylation at the cyclin D2 promoter. *Genes Dev. 15*, 2042–2047.
7. Lin, C. J., Cencic, R., Mills, J. R., Robert, F., and Pelletier, J. (2008) c-Myc and eIF4F are components of a feedforward loop that links transcription and translation. *Cancer Res. 68*, 5326–5334.
8. Eilers, M., and Eisenman, R. N. (2008) Myc's broad reach. *Genes Dev. 22*, 2755–2766.
9. Okubo, T., Knoepfler, P. S., Eisenman, R. N., and Hogan, B. L. (2005) N-myc plays an essential role during lung development as a dosage-sensitive regulator of progenitor cell proliferation and differentiation. *Development 132*, 1363–1374.
10. Hopewell, R., Li, L., MacGregor, D., Nerlov, C., and Ziff, E. B. (1995) Regulation of cell proliferation and differentiation by Myc. *J. Cell Sci., Suppl. 19*, 85–89.
11. Eberhardy, S. R., and Farnham, P. J. (2001) c-Myc mediates activation of the cad promoter via a post-RNA polymerase II recruitment mechanism. *J. Biol. Chem. 276*, 48562–48571.
12. Gomez-Roman, N., Grandori, C., Eisenman, R. N., and White, R. J. (2003) Direct activation of RNA polymerase III transcription by c-Myc. *Nature 421*, 290–294.
13. Lee, T. C., Li, L., Philipson, L., and Ziff, E. B. (1997) Myc represses transcription of the growth arrest gene gas1. *Proc. Natl. Acad. Sci. U. S.A. 94*, 12886–12891.
14. Amati, B., Littlewood, T. D., Evan, G. I., and Land, H. (1993) The c-Myc protein induces cell cycle progression and apoptosis through dimerization with Max. *EMBO J. 12*, 5083–5087.
15. Grandori, C., Cowley, S. M., James, L. P., and Eisenman, R. N. (2000) The Myc/Max/Mad network and the transcriptional control of cell behavior. *Annu. Rev. Cell Dev. Biol. 16*, 653–699.
16. Ayer, D. E., Kretzner, L., and Eisenman, R. N. (1993) Mad: A heterodimeric partner for Max that antagonizes Myc transcriptional activity. *Cell 72*, 211–222.
17. Hurlin, P. J., Queva, C., Koskinen, P. J., Steingrimsson, E., Ayer, D. E., Copeland, N. G., Jenkins, N. A., and Eisenman, R. N. (1995) Mad3 and Mad4: Novel Max-interacting transcriptional repressors that suppress c-myc dependent transformation and are expressed during neural and epidermal differentiation. *EMBO J. 14*, 5646–5659.
18. Zervos, A. S., Gyuris, J., and Brent, R. (1993) Mxi1, a protein that specifically interacts with Max to bind Myc-Max recognition sites. *Cell 72*, 223–232.

19. Nair, S. K., and Burley, S. K. (2003) X-ray structures of Myc-Max and Mad-Max recognizing DNA. Molecular bases of regulation by proto-oncogenic transcription factors. *Cell 112*, 193–205.
20. Choy, B., and Green, M. R. (1993) Eukaryotic activators function during multiple steps of preinitiation complex assembly. *Nature 366*, 531–536.
21. Li, X. Y., Virbasius, A., Zhu, X., and Green, M. R. (1999) Enhancement of TBP binding by activators and general transcription factors. *Nature 399*, 605–609.
22. Holmbeck, S. M., Dyson, H. J., and Wright, P. E. (1998) DNA-induced conformational changes are the basis for cooperative dimerization by the DNA binding domain of the retinoid X receptor. *J. Mol. Biol. 284*, 533–539.
23. Shuai, K., Horvath, C. M., Huang, L. H., Qureshi, S. A., Cowburn, D., and Darnell, J. E., Jr. (1994) Interferon activation of the transcription factor Stat91 involves dimerization through SH2-phosphotyrosyl peptide interactions. *Cell 76*, 821–828.
24. Nair, S. K., and Burley, S. K. (2006) Structural aspects of interactions within the Myc/Max/Mad network. *Curr. Top. Microbiol. Immunol. 302*, 123–143.
25. Sauve, S., Naud, J. F., and Lavigne, P. (2007) The mechanism of discrimination between cognate and non-specific DNA by dimeric b/HLH/LZ transcription factors. *J. Mol. Biol. 365*, 1163–1175.
26. Meier-Andrejszki, L., Bjelic, S., Naud, J. F., Lavigne, P., and Jelesarov, I. (2007) Thermodynamics of b-HLH-LZ protein binding to DNA: The energetic importance of protein-DNA contacts in site-specific E-box recognition by the complete gene product of the Max p21 transcription factor. *Biochemistry 46*, 12427–12440.
27. Ferre-D'Amare, A. R., Prendergast, G. C., Ziff, E. B., and Burley, S. K. (1993) Recognition by Max of its cognate DNA through a dimeric b/HLH/Z domain. *Nature 363*, 38–45.
28. Cohen, S. L., Ferre-D'Amare, A. R., Burley, S. K., and Chait, B. T. (1995) Probing the solution structure of the DNA-binding protein Max by a combination of proteolysis and mass spectrometry. *Protein Sci. 4*, 1088–1099.
29. Hu, J., Banerjee, A., and Goss, D. J. (2005) Assembly of b/HLH/z proteins c-Myc, Max, and Mad1 with cognate DNA: Importance of protein-protein and protein-DNA interactions. *Biochemistry 44*, 11855–11863.
30. Sha, M., Wang, Y., Xiang, T., van Heerden, A., Browning, K. S., and Goss, D. J. (1995) Interaction of wheat germ protein synthesis initiation factor eIF-(iso)4F and its subunits p28 and p86 with m7GTP and mRNA analogues. *J. Biol. Chem. 270*, 29904–29909.
31. Kohler, J. J., Metallo, S. J., Schneider, T. L., and Schepartz, A. (1999) DNA specificity enhanced by sequential binding of protein monomers. *Proc. Natl. Acad. Sci. U.S.A. 96*, 11735–11739.
32. Prendergast, G. C., Lawe, D., and Ziff, E. B. (1991) Association of Myn, the murine homolog of max, with c-Myc stimulates methylation-sensitive DNA binding and ras cotransformation. *Cell 65*, 395–407.
33. Bradford, M. M. (1976) A rapid and sensitive method for the quantitation of microgram quantities of protein utilizing the principle of protein-dye binding. *Anal. Biochem. 72*, 248–254.
34. Laemmli, U. K. (1970) Cleavage of structural proteins during the assembly of the head of bacteriophage T4. *Nature 227*, 680–685.
35. Khan, M. A., Miyoshi, H., Ray, S., Natsuaki, T., Suehiro, N., and Goss, D. J. (2006) Interaction of genome-linked protein (VPg) of turnip mosaic virus with wheat germ translation initiation factors eIFiso4E and eIFiso4F. *J. Biol. Chem. 281*, 28002–28010.
36. Khan, M. A., and Goss, D. J. (2005) Translation initiation factor (eIF) 4B affects the rates of binding of the mRNA m7G cap analogue to wheat germ eIFiso4F and eIFiso4F.PABP. *Biochemistry 44*, 4510–4516.
37. Garland, D. L. (1978) Kinetics and mechanism of colchicine binding to tubulin: Evidence for ligand-induced conformational change. *Biochemistry 17*, 4266–4272.
38. Olsen, K., Christensen, U., Sierks, M. R., and Svensson, B. (1993) Reaction mechanisms of Trp120 → Phe and wild-type glucoamylases from *Aspergillus niger*. Interactions with maltooligodextrins and acarbose. *Biochemistry 32*, 9686–9693.
39. Kohler, J. J., and Schepartz, A. (2001) Kinetic studies of Fos.Jun. DNA complex formation: DNA binding prior to dimerization. *Biochemistry 40*, 130–142.
40. Metallo, S. J., and Schepartz, A. (1997) Certain bZIP peptides bind DNA sequentially as monomers and dimerize on the DNA. *Nat. Struct. Biol. 4*, 115–117.
41. Wendt, H., Thomas, R. M., and Ellenberger, T. (1998) DNA-mediated folding and assembly of MyoD-E47 heterodimers. *J. Biol. Chem. 273*, 5735–5743.
42. Rentzeperis, D., Jonsson, T., and Sauer, R. T. (1999) Acceleration of the refolding of Arc repressor by nucleic acids and other polyanions. *Nat. Struct. Biol. 6*, 569–573.
43. Kim, B., and Little, J. W. (1992) Dimerization of a specific DNA-binding protein on the DNA. *Science 255*, 203–206.
44. Kohler, J. J., and Schepartz, A. (2001) Effects of nucleic acids and polyanions on dimer formation and DNA binding by bZIP and bHLHZip transcription factors. *Bioorg. Med. Chem. 9*, 2435–2443.
45. Park, S., Chung, S., Kim, K. M., Jung, K. C., Park, C., Hahm, E. R., and Yang, C. H. (2004) Determination of binding constant of transcription factor myc-max/max-max and E-box DNA: The effect of inhibitors on the binding. *Biochim. Biophys. Acta 1670*, 217–228.
46. Banerjee, A., Hu, J., and Goss, D. J. (2006) Thermodynamics of protein-protein interactions of cMyc, Max, and Mad: Effect of polyions on protein dimerization. *Biochemistry 45*, 2333–2338.
47. Halford, S. E., and Marko, J. F. (2004) How do site-specific DNA-binding proteins find their targets? *Nucleic Acids Res. 32*, 3040–3052.